Journal of Metals, Materials and Minerals, Vol. 30, No. 1, pp. 73-79, 2020

The luminescence, optical, and structural properties of $SrMoO_4:Ce^{3+}$ phosphor for photonics material applications

Eakgapon KAEWNUAM[1,*], Nuanthip WANTANA[2,3], Sasithorn SAIKAEW[4], and Jakrapong KAEWKHAO[2,3]

[1] *Physics Program, Faculty of Science and Technology, Muban Chombueng Rajabhat University, Ratchaburi, 70150, Thailand*
[2] *Physics Program, Faculty of Science and Technology, Nakhon Pathom Rajabhat University, Nakhon Pathom, 73000, Thailand*
[3] *Center of Excellence in Glass Technology and Materials Science (CEGM), Nakhon Pathom Rajabhat University, Nakhon Pathom 73000, Thailand*
[4] *Center for Science and Applied Science, Faculty of Science and Technology, Muban Chombueng Rajabhat University, Ratchaburi, 70150, Thailand*

[*]**Corresponding author e-mail:** Eakgapon@mcru.ac.th

Received date:
7 September 2019
Revised date:
20 November 2019
Accepted date:
22 November 2019

Keywords:
Phosphors
Luminescence
$SrMoO_4$
Ce^{3+}

Abstract

$SrMoO_4:Ce^{3+}$ phosphors with different Ce_2O_3 concentration were studied in the structure, optical and luminescence properties. The phosphor powders were synthesized by a solid-state reaction to investigate with the XRD, FTIR, absorption and emission spectra measurement. The XRD patterns confirm the tetragonal crystalline structure of $SrMoO_4$ host composition. The FTIR spectra show the dominant vibrations of tetrahedral $[MoO_4]^{2-}$ unit in powders. These phosphors absorb photons in the range of ultraviolet and visible light proved by the absorption spectra. The emission spectra represent the strongest emission at 421 nm wavelength of phosphors under 266 nm excitation. This emission occurred under the transition from the intermediate states between the band gap of $SrMoO_4$ host and its intensity tends to reduce with an increment of Ce_2O_3 concentration due to the perturbation from electron interaction. The $SrMoO_4:Ce^{3+}$ phosphor performs the interesting potential for photonic applications such as ultraviolet to visible light converter and near-ultraviolet / visible light source.

1. Introduction

In present days, the luminescence "phosphor" powder has been applied in various technologies which relates to the light emitting. Some kind of display, lamp, LED, radiation imaging device and radiation detector contain with phosphors. The important factors of efficient phosphor are the strong emission from luminescence center and the useful properties form host material. Several types of phosphor have been studied and developed until now, but there is one that is very interesting, "strontium molybdate doped with lanthanide ion ($SrMoO_4:Ln^{3+}$)". The lanthanide ions (Ln^{3+}) are a group of ions which configure their electrons in 4f level shielded by 5s and 5p. Therefore, the 4f - 4f and 5d - 4f transition of these ions with low perturbation from ligand/crystal field result to the strong emission of ultraviolet (UV), visible light (VIS) and infrared (IR) [1-4]. The luminescence decay time of Ln^{3+} is in the order of millisecond / microsecond (for 4f - 4f transition) and nanosecond (for 5d - 4f) which make Ln^{3+} to be very attractive for various photonic applications. The $SrMoO_4$ compound is a versatile material with non-hygroscopic, high irradiation damage resistance, good thermal and chemical stability [5,6]. In this compound, the distorted tetragonal scheelite-like (β) structure that Mo is coordinated by four O_2 atoms in tetrahedral unit with low phonon energy (~800 cm^{-1}). Moreover, phosphor has strong UV absorption and the absorbed energy can be transferred effectively to the doped Ln^{3+} [7]. These advantages make the $SrMoO_4$ an ideal host for Ln^{3+} doped phosphors. There are many studies and developments of luminescent $SrMoO_4:Ln^{3+}$ phosphors consisting of $SrMoO_4:Eu^{3+}$ [5,8], $SrMoO_4$: Er^{3+}-Yb^{3+} [6], $SrMoO_4:Tb^{3+}$ [9], $SrMoO_4:Sm^{3+}$ [10], $SrMoO_4:Pr^{3+}$ [11], $SrMoO_4:Dy^{3+}$ [12], $SrMoO_4:Tm^{3+}$, Yb^{3+} [13] and $SrMoO_4$: Pr^{3+}/Sm^{3+}, Yb^{3+} [7] for different applications such as white-LED, security ink / latent finger print, solar cell and laser device. However, $SrMoO_4:Ce^{3+}$ phosphor has never been researched. Ce^{3+} is one of Ln^{3+} that its 5d - 4f transition give the UV to blue light emission with highlight yield and nanosecond decay time [4,14,15]. The luminescence characteristic is popularly used in the radiation detector. Then, it is very attractive to investigate $SrMoO_4:Ce^{3+}$ phosphor and discover its possible photonic applications.

In this work, the $SrMoO_4:Ce^{3+}$ phosphors were prepared to study the structure, chemical bonding, optical and luminescence properties. The influence of Ce^{3+} doping amount on these properties were also investigated.

DOI: 10.14456/jmmm.2020.8

2. Experiment method

2.1 Phosphor preparation

$SrMoO_4:Ce^{3+}$ phosphors were prepared by the solid-state reaction with high purity chemicals consisting of $SrCO_3$, MoO_3 and Ce_2O_3. These compounds were prepared together under appropriate stoichiometry and the Ce_2O_3 doped concentration was varied as 0.00, 0.05, 0.10, 0.50, 1.00 and 1.50 mol%. The $SrMoO_4:Ce^{3+}$ phosphor samples then were referred as Ce0.00 (undoped), Ce0.05, Ce0.10, Ce0.50, Ce1.00 and Ce1.50, respectively. Each phosphor sample with 10 g total weight was pressed with 20 tons by hydraulic press machine to make a circle tablet for comfortable measurement. All tablets were annealed with 600°C for 5 h in electrical furnace to make the phosphor nucleation.

2.2 Phosphor measurement

$SrMoO_4:Ce^{3+}$ phosphors were studied the crystalline structure by using x-ray diffractometer (XRD-6100, Shimadzu) with CuKα radiation (0.154 nm wavelength). The chemical bonding of phosphor was investigated via Fourier transform infrared spectrometer (IRrestige-21, Shimadzu). The photon absorption of phosphor was monitored through the absorption spectra by UV-VIS-NIR spectrophotometer (Shimadzu, UV-3600). Phosphors were studied the photoluminescence emission spectra with a spectrofluorophotometer (Cary-Eclipse) using xenon lamp as a light source.

2.3 Data analysis

The strongest peak of XRD results were used to evaluate the crystallite size (t) for each phosphor sample by Debye Scherre's formula,

$$t = \frac{0.89\lambda}{\beta_f \cos\theta} \quad (1)$$

where, λ is the x-ray wavelength using in XRD measurement, β_f and θ is the full width at half maximum (FWHM) and Bragg's diffraction angle of the calculated peaks, respectively [6,8].

The absorption spectra were calculated the optical band gap (E_g) of phosphors following the Wood and Tauc relation,

$$\alpha h\upsilon \propto \left(h\upsilon - E_g\right)^n \quad (2)$$

where, α is the absorbance, h is the Planck constant, υ is the photon frequency, and n can be 1/2, 2, 3/2 or 3 for allowed direct, allowed indirect, forbidden direct and forbidden indirect electronic transitions, respectively [8,9].

3. Results and discussion

3.1 XRD

The XRD results of all $SrMoO_4:Ce^{3+}$ phosphors are shown in Figure 1 (a). The XRD patterns correspond to JCPDs 008-0482 database that confirms the tetragonal structure with $I4_1/a$ space group of host $SrMoO_4$ composition. In this structure, the Mo atom is coordinated by surrounded four O^{2-} ions as tetrahedral $[MoO_4]^{2-}$ unit and each Sr^{2+} ion connects to this unit by occupying the corner with eight adjacent O^{2-} ions of $[MoO_4]^{2-}$ [6,8]. The obvious atomic planes (h k l) in this crystalline structure consist of (1 1 2), (1 1 6), (2 0 0), (2 0 8), (2 0 4), (2 2 0), (0 0 4), (3 1 2) and (2 2 4). The strongest diffraction belongs to (1 1 2) atomic plane centering at 2θ around 27.72°. The diffraction peaks of all phosphor samples are almost similar together due to the small difference of Ce_2O_3 concentration. However, there are very tiny additional diffraction peaks in 2θ between 22.50-26.50° for Ce0.10, Ce1.00 and Ce1.50 phosphors. They possibly represent the structural defect from the rest of $SrCO_3$ that was not reacted completely in the preparation process. This discussion corresponds to the C-O bonding vibration which will be mentioned in the FTIR result. The diffraction data of (1 1 2) atomic plane was used to evaluate the crystallite size in all phosphors using equation (1) as shown the results in Figure 1 (b). The crystallite size of phosphor structure tends to decrease with increasing of Ce_2O_3 concentration, except in Ce0.50 phosphor. The possible explanation is Ce_2O_3 dopant with 0.50 mol% are good incorporated with $SrMoO_4$ host structure and make the crystallite size to be close to the undoped phosphor.

3.2 FTIR

The FTIR transmittance spectra of $SrMoO_4:Ce^{3+}$ phosphors are shown in figure 2. These phosphors absorb the infrared with wavenumber around 784, 991, 1475 and 1679 cm^{-1}. The strongest vibration at 784 cm^{-1} confirms that the main chemical unit in phosphor structure is tetrahedron $[MoO_4]^{2-}$. In the inset figure of FTIR spectra in figure 2, the transmittance of 784 cm^{-1} reduces to minimum point (maximum vibration) when $SrMoO_4$ is doped with 0.05 mol% of Ce_2O_3 and then increases with addition of Ce_2O_3 concentration. The doping of Ce_2O_3 with low concentration as 0.05 mol% possibly improved the construction of $[MoO_4]^{2-}$ unit between the solid-state reaction process, but the doping over than 0.05 mol% degraded this construction. Moreover, the vibration at 784 cm^{-1} also represents the low phonon energy of $SrMoO_4:Ce^{3+}$ phosphor corresponding to one around 800 cm^{-1} of other $SrMoO_4$ phosphors from literature [6]. The low phonon energy of host material can enhance the luminescence ability of

Ln^{3+} dopant [2,16]. The small vibration around 991 and 1475 cm^{-1} exhibits the composition with C-O bonding that is residual from $SrCO_3$ precursor. The very weak vibration of O-H group in phosphor also was found around 1679 cm^{-1} wavenumber.

3.3 Absorption spectra

The absorption spectra of $SrMoO_4:Ce^{3+}$ phosphors are shown in figure 3 (a). These phosphors absorb photons in the range of UV and VIS. For undoped Ce0.00 phosphor, it obviously absorbs the photon with wavelength between 200 - 500 nm under the electronic transition of $SrMoO_4$ band gap only. For Ce^{3+} doped phosphor, there is the additional absorption peak around 352 nm and its absorption strength rises with increment of Ce_2O_3 concentration. Consider to the energy level of Ce^{3+} [14,17], the photon absorption around 352 nm belongs to the 4f - 5d transition of Ce^{3+}. The absorption spectra data in UV range were used to evaluate the optical energy band gap of $SrMoO_4$ phosphor using the Wood and Tauc relation in equation (2). Since the transitions of the molybdates with a scheelite structure exhibit the direct allowed transition, n value in equation (2) is 1/2 and the results are shown in figure 3 (b). From the curves, the band gap energies are determined by the linear extrapolation of the best straight line fit to the hυ (x) axis. The band gap energies of undoped and doped $SrMoO_4:Ce^{3+}$ phosphors are between 4.16 – 4.22 eV which correspond to the band gap of $SrMoO_4:Eu^{3+}$ [8], $SrMoO_4:Tb^{3+}$ [9] and $SrMoO_4$: Tm^{3+}, Yb^{3+} [13] phosphors. There is no obvious relation between the band gap energy of $SrMoO_4:Ce^{3+}$ phosphor and Ce_2O_3 concentration in this work.

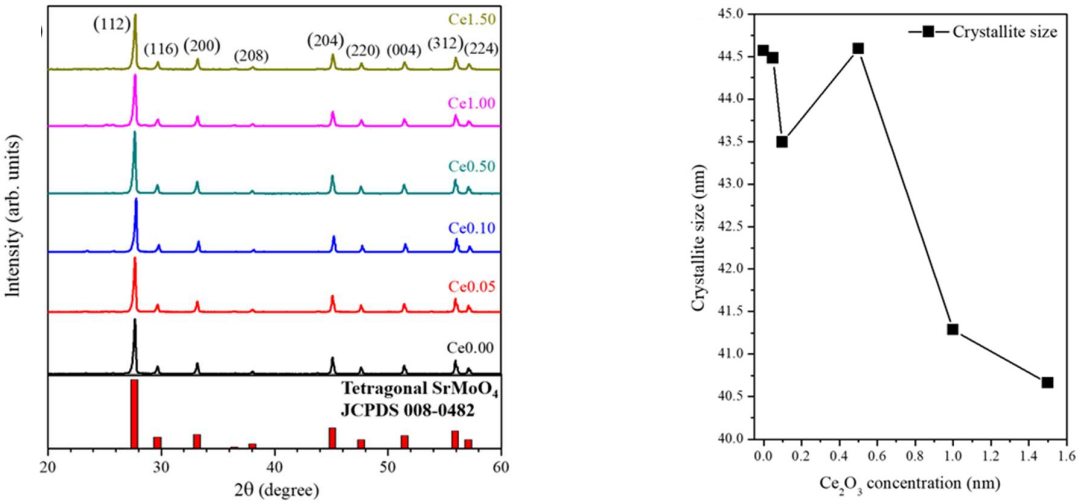

Figure 1. (a) The XRD results of $SrMoO_4:Ce^{3+}$ phosphors compared with XRD pattern from JCPDs 008-0482 database (b) The crystallite size of $SrMoO_4$: Ce^{3+} phosphors as a function of Ce_2O_3 concentration.

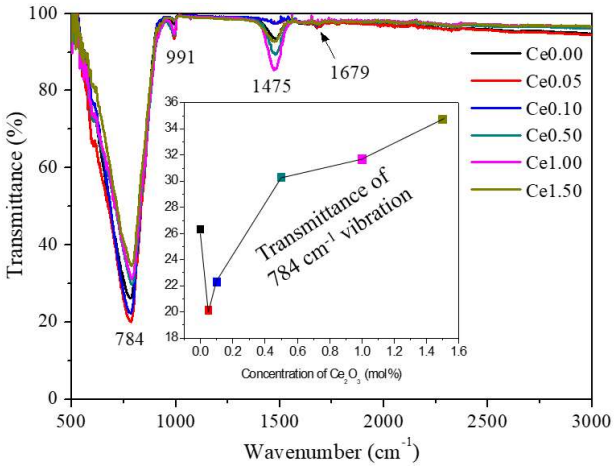

Wavenumber (cm^{-1})	Vibration
784	Mo - O asymmetric stretching vibration in the tetrahedron $[MoO_4]^{2-}$ unit [5-8]
991	C - O stretching vibration [6]
1475	C - O asymmetric stretching vibration [6]
1679	O - H bending vibration [6]

Figure 2. The FTIR spectra of $SrMoO_4:Ce^{3+}$ phosphors with table that show the vibration detail of chemical bonding.

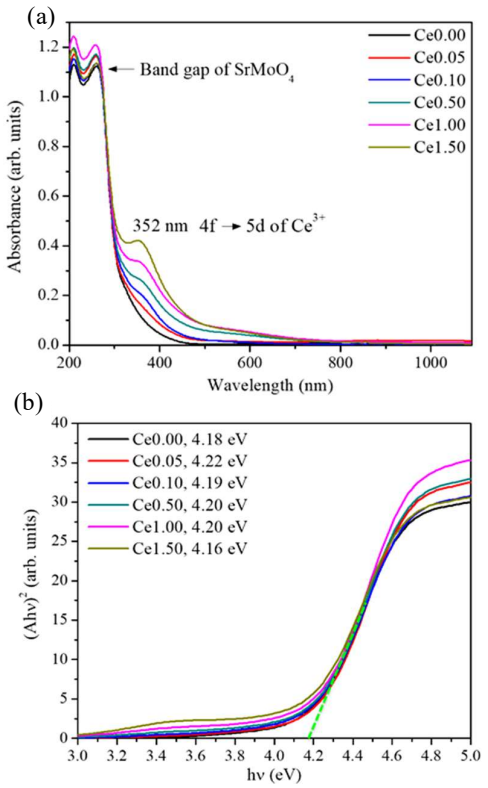

Figure 3. (a) The absorption spectra of $SrMoO_4:Ce^{3+}$ phosphors (b) The $(\alpha h\upsilon)^2$ plot as a function of hυ following Wood and Tauc relation.

3.4 Photoluminescence emission spectra

The doped and undoped $SrMoO_4:Ce^{3+}$ phosphors were monitored the emission spectra under various excitation wavelengths. The target for excitation in this work is $SrMoO_4$ host band gap and 4f - 5d level gap of Ce^{3+}, to investigate the luminescence of Ce^{3+} under energy transfer from $SrMoO_4$ host and Ce^{3+} direct excitation, respectively. Therefore, the first excitation wavelength is 294 nm for 4.22 eV (from Wood and Tauc plot) energy transition crossing the band gap of $SrMoO_4$. The second, third and fourth excitation wavelength is 266 nm, [14], 310 nm [4,15, 18] and 352 nm (from absorption peak and [14]) for the 4f → 5d transition of Ce^{3+}. All emission spectra are shown in Figure 4 (a) – (d) and the possible idea to explain the transition mechanism are in the diagram of Figure 5 (a) and (b). The UV excitation with 294 nm can rise the electron in phosphor from valence to conduction band of $SrMoO_4$ composition (red arrow in Figure 5 (a)). Then, electron energy decays down by non-radiative relaxation (NR) from the conduction band into the energy gap and can occupy in some intermediate states in the gap. The electronic transitions from these intermediate states down to valence band result to the emission with 360 nm, 375 nm, 398 nm and 496 nm for all phosphor sample as shown in spectra in Figure 4 (a). The board peak centering around 496 nm looks like the emission peak of $SrMoO_4$ single crystal reported by Jiang *et al.* [19]. Generally, the emission characteristic of Ce^{3+} under 5d → 4f transition should be the board peak which centers around 328 / 332 nm [15], 345 nm [4,14,15], 356 nm [15], 368 nm [14,18] and 409 nm [14]. But there is no board peak centered around these wavelengths in the spectra, the most nearby wavelengths belong to peak at 360 nm but it is not the board peak. It can be said that there is no the energy transfer process from $SrMoO_4$ host to Ce^{3+} and the luminescence come only from the intermediate states of $SrMoO_4$. This radiation intermediate state in $SrMoO_4$ band gap possibly is the vibration ground state of excited charge transfer, O^{2-} 2p → Mo^{6+} 4d, band in MoO_4^{2-} unit. Li *et al.* [13] mentioned about the Stoke shift that relaxes the transferred electron down to this vibrational state before it produces the blue emission. This corresponds to our some emission peaks in blue light region. Moreover, these intermediate states perhaps originate from the defect or some impurities contained in $SrMoO_4$. Park *et al.* calculated the band structure and density of states (DOSs) of $SrMoO_4$ composition [9]. The theoretical calculation performs an intermediate state of oxygen vacancy defect which locates around 2.09 eV over than the conduction band.

The emission spectra of $SrMoO_4:Ce^{3+}$ phosphor with 266 nm excitation are shown in Figure 4 (b). The intention for using this excitation wavelength is the direct excitation to Ce^{3+} for luminescence production. However, these spectra still do not show the board emission peak of Ce^{3+}. As shown in Figure 5 (a), some 5d levels of Ce^{3+} overlap to the conduction band of $SrMoO_4$ since the energy is higher than 34,013 cm^{-1}. In theory, the 226 nm excitation (37,584 cm^{-1}) can excite simultaneously the electron of $SrMoO_4$ host to its conduction band and the electron of Ce^{3+} to its 5d level (blue arrow in Figure 5 (a)). In practically, electron in Ce^{3+} is excited with very small probability due to low concentration of Ce_2O_3 in phosphor. Therefore, almost all of UV energy at 266 nm excites the electron in $SrMoO_4$ to rise up to the conduction band and decay down to the intermediate states with similar process to the 294 nm excitation. The emissions then originate from the intermediate states of $SrMoO_4$ only, not from 5d level of Ce^{3+}. The obvious emission peak under 266 nm excitation centers around 296 nm, 310 nm, 361 nm, 421 nm and 492 nm. In Figure 4 (c), the UV excitation with 310 nm results to the emission spectra which also do not show any board peak of Ce^{3+}. The obvious emission peak centers around 360 nm, 376 nm, 421 nm and 487 nm corresponding to the emission peak under previous both excitations. Therefore, these emissions also come from the intermediate states in $SrMoO_4$ band gap. Due to low Ce_2O_3 doped concentration and excitation energy with 310 nm lower than $SrMoO_4$ band gap, almost all of this excitation energy rises the electron in $SrMoO_4$ up to an intermediate state around 32,258 cm^{-1} over than the valence band (blue arrow in Figure 5 (b)). Then, the NR processes and those emission transitions of the intermediate states occur respectively. The emission

spectra under 352 nm excitation wavelength are performed in Figure 4 (d) with lack of the strong emission peak. Look back at the absorption spectra, there is an absorption peak around 352 nm under 4f → 5d transition of Ce^{3+}. The absorbed energy mostly disappears without the luminescence of Ce^{3+}. For the possible explanation, the electron of Ce^{3+} is excited to 5d level (red arrow in Figure 5 (b)) and the excited energy transfer from 5d level to the non-radiation intermediate state (state with dash line) in $SrMoO_4$ band gap. Then, the energy in this intermediate state is released in a term of thermal vibration by NR process.

Consider the spectra in each Figure 4 (a), (b) and (c) the intensity of emission peak tends to decrease with increment of Ce_2O_3 concentration. Since the 5d electronic level of Ce^{3+} possess the range of energy from inside band gap to the conduction band of $SrMoO_4$, the addition of Ce_2O_3 into phosphor make an electron interaction between 5d level of Ce^{3+} versus state of conduction band / intermediate state in band gap of $SrMoO_4$. This perturbation from Ce^{3+} results to the reduction of emission intensity. For comparison the emission strength among different excitation wavelength, the UV excitation with 266 nm produces the strongest emission at 421 nm from intermediate states of $SrMoO_4$, while the excitation with 352 nm produces the very weak emissions signal which cannot be identified the source. Overall results of photoluminescence perform the strong near-UV and VIS emission of phosphors under UV excitation which can be applied in UV to VIS converter and near-UV / VIS source.

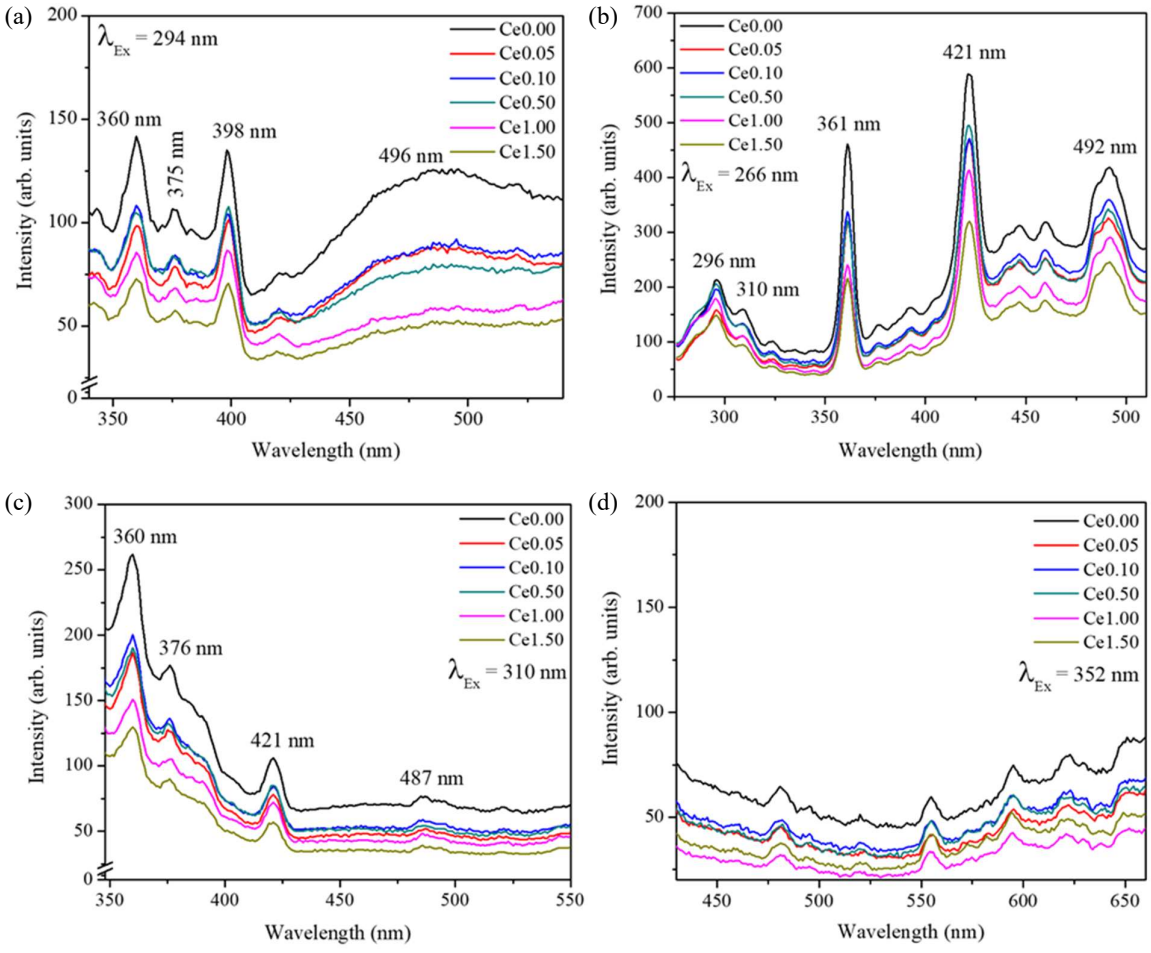

Figure 4. The emission spectra of $SrMoO_4:Ce^{3+}$ phosphors under excitation with (a) 294 nm, (b) 266 nm, (c) 310 nm and (d) 352 nm wavelength.

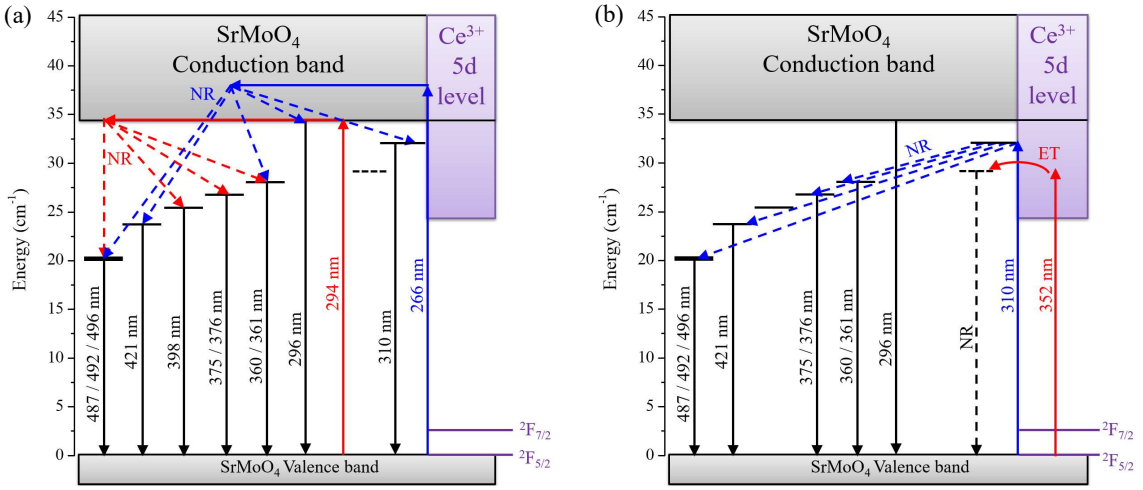

Figure 5. The energy level diagram of $SrMoO_4:Ce^{3+}$ phosphors for emission spectra under excitation with (a) 294 nm and 266 nm and (b) 310 and 352 nm wavelength. The short horizontal solid/dash lines represent the radiation/ non-radiation intermediate states. The solid arrows represent the energy transitions or migrations while the dash ones represent the non-radiative relaxation process.

4. Conclusions

$SrMoO_4:Ce^{3+}$ phosphors, prepared by the solid-state reaction, possess the main crystal structure of tetragonal with $I4_1/a$ space group. Ce_2O_3 dopant with 0.50 mol% are good incorporated with $SrMoO_4$ host structure and make the crystallite size to be close to undoped phosphor. The dominant chemical unit in phosphor is $[MoO_4]^{2-}$ which was best constructed in 0.05 mol% Ce_2O_3 doped phosphor. Ultraviolet radiation was absorbed by the energy band gap of $SrMoO_4$ host and the 4f-5d electronic gap of Ce^{3+} dopant. Ultraviolet excitations with 294 nm, 266 nm and 310 nm generate the obvious emissions from intermediate states in the $SrMoO_4$ band gap without the emission from 5d-4f transition of Ce^{3+}. The strongest emission belongs to visible light with 421 nm under 266 nm excitation. The emission intensity of $SrMoO_4$ tends to reduce with an increment of Ce_2O_3 concentration due to the perturbation from electron interaction. The $SrMoO_4:Ce^{3+}$ phosphor performs the interesting potential for photonic applications such as ultraviolet to visible light converter and near-ultraviolet/visible light source.

5. Acknowledgements

The authors with to thank Center of Excellence in Glass Technology and Materials Science (CEGM) Nakhon Pathom Rajabhat University (NPRU) and Muban Chombueng Rajabhat University for research facilities.

References

[1] B. G. Wybourne, *Spectroscopic properties of rare earths*. New York: John Wiley & Sons., 1965.

[2] G. C. Righini and M. Ferrari, "Photoluminescence of rare-earth–doped glasses," *La Rivista del Nuovo Cimento*, vol. 28, no. 12, pp. 1-53, 2006.

[3] N. Wantana, E. Kaewnuam, Y. Ruangtaweep, D. Valiev, S. Stepanov, K. Yamanoi, H. J. Kim, and J. Kaewkhao, "Radio, cathodo and photoluminescence investigations of high density WO_3-Gd_2O_3-B_2O_3 glass doped with Tb^{3+}," *Radiation Physics and Chemistry*, vol. 164, 108350, 2019.

[4] N. Wantana, E. Kaewnuam, N. Chanthima, S. Kaewjaeng, H. J. Kim, and J. Kaewkhao, "Ce^{3+} doped glass for radiation detection material," *Ceramics International*, vol. 44, pp. S172-S176, 2018.

[5] A. P. A. Marques, M. T. S. Tanaka, E. R. Leite, and I. L. V. Rosa, "The Role of the Eu^{3+} Concentration on the $SrMoO_4$:Eu Phosphor Properties: Synthesis, Characterization and Photophysical Studies," *Journal of Fluorescence*, vol. 21, no. 3, pp. 893-899, 2011.

[6] A. K. Soni and V. K. Rai, "$SrMoO_4:Er^{3+}$-Yb^{3+} upconverting phosphor for photonic and forensic applications," *Solid State Sciences,* vol. 58, pp. 129-137, 2016.

[7] W. Xia, S. Xiao, X. Yang, and X. Jin, "Quantum cutting and tunable luminescence properties in Pr^{3+}/Sm^{3+}, Yb^{3+} co-doped $SrMoO_4$ powders," *Materials Research Bulletin*, vol. 89, pp. 5-10, 2017.

[8] C. Shivakumara and R. Saraf, "Eu^{3+}-activated $SrMoO_4$ phosphors for white LEDs applications: Synthesis and structural characterization," *Optical Materials*, vol. 42, pp. 178-186, 2015.

[9] S. W. Park, B. K. Moon, J. H. Jeong, J. S. Bae, and J. H. Kim, "Crystal structure, electronic structure, and photoluminescent properties of

SrMoO4:Tb^{3+} phosphors," *Materials Research Bulletin*, vol. 70, pp. 403-411, 2015.

[10] X. Lin, X. Qiao, and X. Fan, "Synthesis and luminescence properties of a novel red $SrMoO_4:Sm^{3+},R^{+}$ phosphor," *Solid State Sciences*, vol. 13 , no. 3, pp. 579-583, 2011.

[11] F. Chun, B. Zhang, H. Su, H. Osman, W. Deng, W. Deng, H. Zhang, X. Zhao, and W. Yang, "Preparation and luminescent properties of self-organized broccoli-like $SrMoO_4$: Pr^{3+} superparticles," *Journal of Luminescence*, vol. 190, pp. 69-75, 2017.

[12] X. Li, L. Guan, M. Sun, H. Liu, Z. Yang, Q. Guo, and G. Fu, "Luminescent properties of Dy^{3+} doped $SrMoO_4$ phosphor," *Journal of Luminescence*, vol. 131, no. 5, pp. 1022-1025, 2011.

[13] L. Li, Y. Pan, W. Chang, Z. Feng, P. Chen, C. Li, Z. Zeng, and X. Zhou, "Near-infrared downconversion luminescence of $SrMoO_4$: Tm^{3+}, Yb^{3+} phosphors," *Materials Research Bulletin*, vol. 93, pp. 144-149, 2017.

[14] A. Bahadur, Y. Dwivedi, and S. B. Rai, "Optical properties of cerium doped oxyfluoroborate glass," *Spectrochimica Acta Part A: Molecular and Biomolecular Spectroscopy*, vol. 110, pp. 400-403, 2013.

[15] J. Zhong, H. Liang, H. Lin, B. Han, Q. Su, and G. Zhang, "Effects of crystal structure on the luminescence properties and energy transfer between Gd^{3+} and Ce^{3+} ions in $MGd(PO_3)_4:Ce^{3+}$ (M = Li, Na, K, Cs)," *Journal of Materials Chemistry*, vol. 17, no. 44, pp. 4679-4684, 2007.

[16] J. García Solé, L.E. Bausá, and D. Jaque, *An Introduction to the Optical Spectroscopy of Inorganic Solids*. England: John Wiley & Sons Ltd., 2005.

[17] Q. Wang, S. Ouyang, W. Zhang, B. Yang, Y. Zhang, and H. Xia, "Luminescent properties of Ce^{3+}-doped transparent oxyfluoride glass ceramics containing $BaGdF_5$ nanocrystals," *Journal of Rare Earths*, vol. 33, no. 1, pp. 13-19, 2015.

[18] M. Ajmal, T. Alib, S. A. Mian, M. A. Khan, S. Ahmad, and A. A. Khana, "Effects of Ce^{3+}-doping concentration on the luminescent properties of $La_2O_3:Ce^{3+}$ phosphors," *Materials Today: Proceedings*, vol. 4, no. 3, pp. 4924-4929, 2017.

[19] H. Jiang, G. Rooh, H. J. Kim, H. Park, J. H. So, S. Kim, S.K. Kim, Y.D. Kim, and W. Zhang, "Growth and Scintillation Characterizations of $SrMoO_4$ Single Crystals," *Journal of the Korean Physical Society*, vol. 63, no. 10, pp. 2018-2023, 2013.